SCIENTIFIC CULTURE
www.sci-cult.com

SCIENTIFIC CULTURE, Vol. 12, No. 4, (2026), pp. 1694-1704
Open Access. Online & Print

DOI: 10.5281/zenodo.12426250

COMPARATIVE ANALYSIS OF BER PERFORMANCE FOR RS, CONVOLUTIONAL, LDPC, AND TURBO CODES IN UNDERWATER ACOUSTIC COMMUNICATION CHANNELS

Chetan Naik J[1]*, Abdul Haq Nalband[2]

[1]Research Scholar, School of ECE, Reva University, Bangalore, India. Email: chetanmassand@gmail.com
[2] Associate Professor, Department of CSE (AI & ML), Dayananda Sagar University, Bangaluru South, Karnataka, India. Email: abjag.n@gmail.com

Received: 15/08/2025
Accepted: 22/02/2026

Corresponding Author: Chetan Naik J (chetanmassand@gmail.com)

ABSTRACT

The use of sound communication underwater (UWAC) is crucial for expeditions, surveillance, and resource management, but it is severely constrained by multipath propagation, Doppler spread, restricted data transfer capacity, and interference between symbols (ISI). Coding channels are a vital technique to improve reliability under such harsh conditions. In this study, we compare the bit error rate (BER) performance of four different types of codes: convolutional, RS, Turbo, and LDPC, along with a hybrid RS→π→Convolutional scheme with erasures, in simulated underwater acoustic channels. The evaluation is conducted using MATLAB R2024b across three transform domains— Wavelet Transform with Dual Trees (DTCWT), Wavelet Transform with Discretes (DWT), and Fast Fourier Transform (FFT)—to capture diverse channel behaviours. Performance metrics include average BER, BER at 6 dB, and the area under log10(BER) curves. Simulation results demonstrate that the hybrid coding scheme consistently outperforms all other approaches, achieving the lowest BER and best area performance across domains, with especially strong gains at higher SNR values. Convolutional codes emerge as a close second, while LDPC provides stable and reliable results. Turbo codes show competitive but less consistent behaviour, and RS-only and uncoded BPSK schemes yield weaker performance except in very high-SNR scenarios. Overall, the study highlights the practical advantage of hybrid concatenated coding strategies in achieving robust, efficient, and adaptive UWAC, offering significant improvements for future underwater communication systems.

KEYWORDS: Underwater Acoustic Communication (UWAC), Bit Error Rate (BER), Reed–Solomon (RS) codes, Convolutional codes, Turbo codes, LDPC codes, Hybrid coding, DTCWT, DWT, FFT, MATLAB R2024b.

1. INTRODUCTION

The seas are strategically and economically significant because they contain resources that enable human growth and survival; they also span 71 percent of the planet's surface. The rapid development of fishing, environmental surveillance, marine engineering, academic study, and the protection of interests and rights in the maritime domain has necessitated the collecting and dissemination of marine data an important and valuable part of maritime activities [1,2]. However, for a long time, many countries' marine scientific and technology efforts have been obstructed by the difficulty of gathering and conveying marine data in complicated maritime ecosystems.

Underwater wireless communication over long distances is best accomplished via acoustic waves due to their low attenuation in saltwater [3]. It is essential and practical to use auditory communication technique for reliable, high-speed data transmission transfer due to the diverse spectrum of maritime operations. Nevertheless, there is a wide range of marine environmental elements that may alter the structure of the underwater acoustic (UWA) channel, including wind direction and speed, temperature, water velocity, wind waves, internal waves, and topographical features. This causes difficulties with underwater acoustic communication (UWAC) such as a narrow bandwidth, frequency-selective fading, low coherence durations, and intense interference between symbols (ISI) [4]. The UWA channel's intricate features make it difficult to create communication systems that are stable, dependable, and ecologically sound.

As a crucial component of the UWACS architecture, channel coding—along with channel estimation and equalization—is a vital tool in the fight against ISI caused by differences in the UWA channel hierarchy. Through the use of interleaving algorithms to rectify random burst mistakes caused by complex channels and include extra bits in the transmitted data, channel coding provides different degrees of safety. Recently, Because of the expansion of channel-coding techniques have hit the Shannon limit in information theory. One important area of study for the revolutionary improvement of UWAC technology is the combination of UWAC with sophisticated channel coding algorithms. This will allow for the transmission of marine data of high quality across a variety of channel topologies ratios of signals to noise (SNR) [5].

At the moment, UWAC often employs channel coding techniques examples of which are RS codes [6], convolutional codes [7], the well-studied turbo codes [8], and LDPC [9], whose efficiency is almost to Shannon's limit. Theoretically, polar codes in B-DMCs, which are discrete memoryless channels with binary input/output may reach Shannon's limit [10]. It's important to note that the polar, LDPC, and turbo codes function better with longer code lengths. But wherever feasible, The UWA channel, which is a data blocks must be shorter in order to accommodate the spatial-temporal frequency variable. Research integrating finite code length coding methods with UWA channel characteristics is thus essential for more investigation in real-world applications.

Furthermore, the maritime environment's complexity and variety cause Modifications to the UWA channel's multi-path structure Furthermore, the unpredictability of its timing poses a serious threat to the reliability of data transfer in the UWACS. Lately, researchers have focused on improving UWAC performance in areas like as responsiveness to changes in propagation, latency, and bandwidth efficiency circumstances [11]. In wireless communications, rate-compatible coding techniques are often used to flexibly control the rates and durations of various codes using puncturing. Transmission across channels with different bit error rates may be done efficiently using this method. Furthermore, this method may improve transmission dependability overall, which is important for a lot of communication applications [12].

A rate-compatible channel coding system channel estimate and the UWA channel's spatiotemporal frequency fluctuation enable the oceanic channel's unique characteristics to inform the adjustment of channel coding rates and lengths. For instance, low bit rate channel coding could be required to accomplish certain performance goals when the channel's signal-to-noise ratio (SNR) is low, and vice versa when the SNR is high, the channel may make use of longer and more robust code rates. Here, we look analyze how well turbo, LDPC, convolutional, and RS codes handle bit error rates (BERs) in underwater acoustic communication channels, highlighting their effectiveness and limitations under varying UWA conditions.

2. RELATED WORK

Zhao et al., [13] reviews and compares research on focused on actual performance in shallow water situations under real noise utilizing examples of which are polar codes and LDPC. Environmental noise, multi-path influences, and Doppler make it difficult to design a reliable UWACS. An effective

option is channel codes, which exhibit minimal complexity while yet reaching Shannon's capacity. By finding a happy medium rate-compatible codes are able to provide smooth rate-adaptive transmission under different conditions by balancing communication efficiency with channel tolerance channels. Liu et al., [14] introduced a method for decoding and equalization that cycles across combat intersymbol interference in underwater acoustic environments. It uses creates an EXIT-assisted strategy for LDPC code optimization using extrinsic information transfer charts for LDPC code performance analysis. Optimized codes work better than standard or Turbo codes, according to computer simulations, with gains of 1.0 and 0.8 dB.

Benxue et al., [15] proposes a communication system scheme that integrates low code rate LDPC coding with multicarrier MFSK (MC-MFSK) in shallow water channels. It addresses the mismatch between LDPC standard code rate and hydro acoustic harsh environments by generating low code rate LDPC codes through base matrix expansion. The low-bitrate LDPC code performs better than convolutional codes, according to the simulation findings and Hadamard-Convolution joint codes. The reliability of the proposed communication scheme is verified through a shallow sea experiment in Wuyuan Bay, China. [16] examines Turbo codes, polar codes, and linear gradient pseudocodes all perform well in a white Gaussian additive noise channel with inter symbol interference. To mitigate the interference, an equalizer was employed at the receiver's level. These equalizers were MMSE and ZF, or minimum mean square error and zero forcing, respectively. Our performance measure was the change in bit error rate relative to the signal-to-noise ratio. This research adds to the literature on digital communications by investigating equalization within the context of turbo codes, namely LDPC codes and polar codes.

Pelekanakis et al., [17] evaluates the efficacy of FEC codes for error correction in improving underwater acoustic communications. It uses in-situ data from six FEC codes and examines two common payload sizes. The analysis uses single-carrier Transmissions of Keying phases in a high-north environment. The optimal channel replay framework is developed using a Decision Feedback Equalizer Based on Channel Estimate, where at the very top of the performance scale is the polar code. Modernizing the equalizer with a turbo feature can further reduce PER. According to [18] the main challenge where UWA stands for undersea acoustic communication, the BER, which significantly impacts communication. This paper investigates various coding schemes, including Equipped with Turbo, LDPC, Convolution, the t-distribution noise channel, and Polar coding are implemented. The evaluation considers binary phase-shift keying (BPSK) modulation with a 1/2 code rate. The results show Polar coding outperforms alternative UWA channel coding techniques as a result of lower BER and computational complexity.

3. CHANNEL CODES FOR UWAS

One-way channel coding guarantees security is by lowering the bit error rate (BER) when sending data across a noisy channel. by providing redundant data bits transferred via constraint relations. In UWA communications, it is a powerful weapon against ISI. Here we go over the two primary coding methods utilized in UWA communication technology development and research: fixed-rate and rate-compatible.

3.1 Reed Solomon (RS) Code

Applications for Solomon Reed Among the many uses for error-correcting codes is the transfer of data aboard spacecraft in route to or from deep-space missions to retrieving data by the ubiquitous use of QR codes and bar codes. In their 1959 publication “Polynomial Codes over Certain Finite Fields” appears in the JSOM Journal, written. The productions of Irving Reed and Gus Solomon work shared the Reed Solomon (RS) Code with the world. Since then, RS Codes have played a crucial role in the revolution in telecommunications things happened towards the century's end.

Because Digital error control codes that are most often used are Reed-Solomon codes, which are used wherever in the globe where non-volatile memory and computer memory are used. A few key applications are as follows Computer Memory, Feedback Error Control for Digital Audio Disc, Deep Space Telephony, and Spread-Spectrum Systems. Applying the symbols of the 2m-dimensional Galois field GF (i.e., q = 2m) and, we examine Reed-Solomon codes. Let GF(2m) contain a primitive element. A basic terror-correcting Reed-Solomon code using a generating polynomial 2 meters in length, which is

$$g(X) = (X+A)(X+A^2) \cdots (X+A^{2t}) = g_0+g_1X+g_2X^2+\cdots+g_{2t-1}X^{2t-1}+X^{2t} \quad (1)$$

Polynomials with coefficients from GF(2m) that are multiples of g(X) and having degrees of n - 1 or less make up the (n, n – 2t) Cyclic code that is produced by g(X). This code's encoding is comparable to that of the binary case [19].

3.2 Convolutional codes

3.2.1 Encoding

A straightforward mix of memory components and XOR operations can be used to efficiently convolve the input bits with the code polynomials. The LTE rate 1/3 convolutional encoder, which describes the polynomials (Gi) in octal form, is depicted in Fig. 1 [20]. Decoding later on requires an understanding of the states' transitions. Additionally, the decoder needs to know the encoder's beginning and ending states in order to avoid performance loss. Convolutional codes benefit from low encoding complexity due to their straightforward structure, and when paired with the rapid clock speeds of the most advanced systems, encoding lag is eliminated.

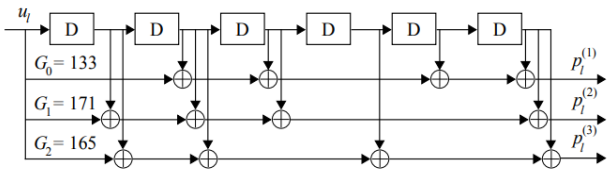

Fig 1: LTE rate 1/3 convolutional encoder

3.2.2 Decoding

We take into consideration the BCJR algorithm-based bit-wise decoder for Maximum A Posteriori (MAP) [21]. The information bit u_1's log-likelihood ratio (LLR) at time l, after receiving codeword y and decoding bit $\hat{u}_l$, is provided by

$$L_{u_l} = \log\left(\frac{P\{u_l=0|y\}}{P\{u_l=1|y\}}\right) \quad (2)$$

Since convolutional codes have a Trellis structure, these probabilities may be expressed as [22]

$$L_{u_l} = \log\left(\frac{\sum_{U_0} P\{s_{l-1}=s', s_l=s, y\}}{\sum_{U_0} P\{s_{l-1}=s', s_l=s, y\}}\right) (3)$$

where s_l is the state at time l, and U_0 is the collection of all possible pairings (s', s_l) for the state transition s' → s when $u_l = 0$, and U_1 is the set of pairs (s', s_l) for the transition when $u_l = 1$. These probabilities may be factorized using the BCJR technique as

$$P\{s_{(l-1)} = s', s_l = s, y\} = \alpha_{l-1}(s')\, \gamma_l(s', s_l)\, \beta_l(s) \quad (4)$$

where $\gamma_l(s', s_l)$ represents the Branch Metric. The terms α_{l-1} and β_l go through a series of iterative calculations. With this process, the log domain is used, where the LLR's final expression is determined by [22]

$$L_{u_l} = (\max^*_{U_0}[\alpha_{l-1}(s') + \gamma_l(s', s_l) + \beta_l(s)] - (\max^*_{U_1}[\alpha_{l-1}(s') + \gamma_l(s', s_l) + \beta_l(s)]) \quad (5)$$

The max* function is given by

$$\max^*(a, b) = \max(a, b) + \log(1 + e^{-|a-b|}) \quad (6)$$

A technique that is based on the Max-Log-MAP approach is the approximation that is achieved by ignoring the log term [23].

3.3 Turbo codes

Typically, an interleaver separates two recursive convolutional encoders, which are then combined to produce turbo codes. The next stage is to use the appropriate interleaver and generate code polynomials for every encoder.

3.3.1 Encoding

The same conversation we had in the last part continues here because each encoder functions primarily as a convolutional layer. In a network, the interleaver is the only new component. Figure 2 illustrates the turbo encoder utilised in LTE [24], which employs an interleaver based on Quadratic Permutation Polynomials (QPP). A parity stream is produced by the first encoder $p1^{(1)}$and a systematic stream u1, but the second encoder just produces a parity stream $p1^{(2)}$. It is a rate 1/3 turbo code as a result.

In a similar vein, in order to prevent performance degradation, it is critical to know the beginning encoder beginning and finishing states at decoder. Trellis termination is used to manage this.

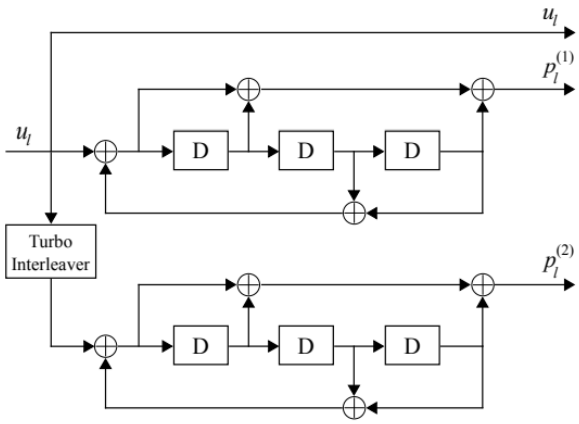

Fig 2: LTE rate 1/3 turbo encoder

3.3.2 Decoding

Turbo decoders are really two SISO decoders working together. Equipped with a few exceptions, those decoders are comparable to convolutional decoders. The first decoder receives one parity stream and one systematic stream, and the second one receives an additional parity stream in addition to the systematic stream in an interleaved form. As soon as the first decoder runs, it produces extrinsic information, which is a cleaned-up version of the final LLR.

The second decoder receives this interleaved. It carries out decoding, which is more dependable than in the event that it lacks the extra information retrieved this decoder's output. It works in a similar way by creating external data for the first decoder

and, instead of interleaving, deinterleaves to show that an iteration is over.

Although it begins in a similar fashion to the prior iteration, the first decoder now uses the second decoder's extrinsic data, resulting in accurate calculation of the output.

Until a halting requirement is met When completing the decoding procedure by reaching the maximum allowed number of repetitions keeps going.

Following each repetition, the overall LLR is determined by [18]

$$L_{u_{l(total)}} = L_{u_{l(channel)}} + L_{u_{Deint(l)}}^{e(2\to1)} + L_{u_l}^{e(1\to2)} \quad (7)$$

where $L_{u_{l(channel)}}$ is the channel LLR, $L_{u_{Deint(l)}}^{e(2\to1)}$ is u_l transferred from the first decoder to the second, which is external, and Deint(l) is the location of the uninterleaved u_l.

The original and interleaved streams would seem to be uncorrelated if the interleaver was properly built. Since neither the original stream nor its interwoven version is likely to undergo the identical encoding, gearbox and/or decoding conditions, this is crucial for the turbo gain.

3.4 LDPC codes

One way to recognize seeking out a sparse parity check matrix is the way an LDPC code is generated. Due to the lack of may be used to facilitate encoding and decoding of low complexity. Displayed above is a code snippet:

$$H = \begin{bmatrix} 1 & 1 & 0 & 0 & 1 & 0 \\ 1 & 0 & 1 & 1 & 0 & 0 \\ 0 & 0 & 1 & 0 & 1 & 1 \\ 0 & 1 & 0 & 1 & 0 & 1 \end{bmatrix} (8)$$

It is provided here merely as an example. The LDPC codes may be shown visually using a Tanner graph [25]. The columns represented by Variable Nodes (VNs), and the rows by Check Nodes (CNs). Each "1" in the matrix represents a connection between a CN and a VN. An example of a Tanner graph in code is displayed in Fig. 3.

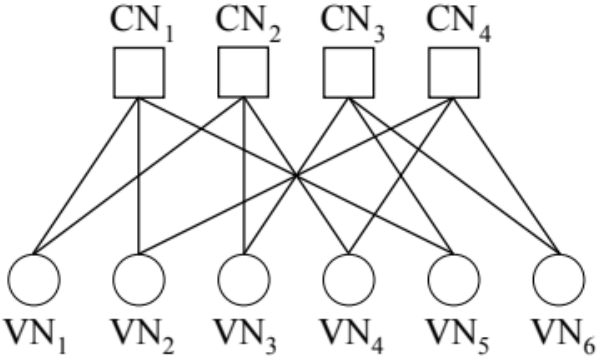

Fig 3. Tanner graph of the example code.

3.4.1 Encoding

The encoding may be explained as follows:

$$c = uG \quad (9)$$

The generator matrix G, the input block u, and the output codeword c are defined here.

The design parameter for LDPC codes is defined by the parity check matrix H and the generating matrix G. Nonetheless, the generator matrix may be derived from a parity check matrix that is provided. Typically, this is accomplished by systematically using Gauss-Jordan Elimination to transform H into a form that can be directly used to find the generating matrix.

The parity check matrix only works with a certain length of input blocks; it won't work with any other lengths. That's the first of two issues. As a second issue, the process of transforming Simplifying H into a systematic form could make it unsuitable for very large block lengths. To tackle the first problem, we use Quasi-Cyclic (QC) LDPC codes, which are quite flexible in terms of input size due to Lifting [26].

Avoiding an approach resembling Repeat-Accumulate (RA) codes may be used to solve the second problem; this structure enables the parity check matrix to be encoded directly by back substitution.

3.4.2 Decoding

The with the use of the Sum Product Algorithm, LDPC codes may be deciphered. The fact that The CNs and VNs in the Tanner graph are interacting with each other leads to this conclusion. Before anything else, the VNs communicate with the linked CNs via channel LLRs Lj. The CNs thereafter carry out the computation and communicate new messages to their linked VNs in accordance with [22].

$$L_{(i\to j)} = 2\tanh^{-1}\left(\prod_{j\prime\in N(i)\setminus\{j\}} \tanh\left(\frac{L_{j'\to i}}{2}\right)\right) \quad (10)$$

Where $L_{i\to j}$ is the message passed from the i^{th} CN to the j^{th} VN, $L_{j'\to i}$ represents the information sent from the j^{th} virtual network node to the i^{th} connected node, and N (i) is the collection of virtual networks linked to the i^{th} node. Once the VNs have received and processed these messages, they will relay new messages to the associated CNs in accordance with.

$$L_{(j\prime\to i)} = L_j + \sum_{i\prime\in N(j)\setminus\{i\}} L_{(i\prime\to j)} \quad (11)$$

Performance may be impacted by the order the order in which the nodes are planned. The aforementioned Flood timetable is the one in which every CN is update their messages simultaneously, followed by all VNs. Performing serial scheduling can result in better performance. This method, known as Layered Belief Propagation (LBP) [27], provides nearly increase the convergence pace by two times in comparison to the flood schedule, measured in iterations.

$$L_{(i\to j)} = \left(\prod_{j'\in N(i)\setminus\{j\}} \alpha_{j'\to i}\right).\min_{j'\in N(i)\setminus\{j\}} \beta_{j'\to i} \quad (12)$$

where $\alpha_j'\to i$ and $\beta_j'\to i$ are the sign and magnitude of $L_j'\to i$, that is, in their own right. While this Min-Sum approximation does reduce complexity in decoding, it does so at the expense of efficiency.

3.5 Hybrid RS–Convolutional Codes

Hybrid RS–Convolutional coding integrates Reed–Solomon (RS) codes with convolutional codes to exploit the complementary strengths of both. The outer RS code provides strong burst-error correction at the symbol level, while the inner convolutional code offers robust protection against random errors. The overall code the hybrid scheme's rate is equal to the sum of the two separate rates.

$$Rtot = RRS \times Rconv \quad (13)$$

Were

$$R_{RS} = \frac{k}{n}, R_{conv} = \frac{K}{N} \quad (14)$$

Here, The RS code message is k characters long, and the RS code codeword is n. (in symbols), while K and N represent the bits used by the convolutional encoder for input and output, respectively.

3.5.1 Encoding

Let the binary information sequence be represented as

$$u = [u_1, u_2, \ldots, u_L] \quad (15)$$

where $L = k \cdot m \cdot N_{cw}$, with m denoting the number of bits used by each RS symbol, and N_{cw} the number of RS codewords per frame.

RS Encoding

The input sequence is grouped into RS symbols in $GF(2^m)$, and then encoded into an RS codeword.

$$c_{RS} = u \cdot G_{RS} \quad (16)$$

where G_{RS} serves as the RS code's generating matrix. It is possible to correct up to a (n, k) RS code.

$$t = \frac{n-k}{2} \quad (17)$$

symbol errors per codeword.

Interleaving

The serialized RS-The bits that are encoded are randomly or sequentially shuffled using an interleaver.

$$b_{int} = \pi\, c_{RS} \quad (18)$$

Where $\pi(\cdot)$ denotes the interleaving operation.

Convolutional Encoding

The interleaved bits are passed through the convolutional encoder, producing

$$cconv = bint \cdot Gconv \quad (19)$$

Where G_{conv} represents the convolutional generator polynomial. The output is then transmitted over the channel.

3.5.2 Decoding

At the receiver, the decoding process reverses the above steps:

Convolutional Decoding

Received noisy symbols are first processed by a Viterbi decoder, which computes

$$\hat{b}_{int} = \arg\max_b P(y|b, G_{conv}) \quad (20)$$

with y representing the received sequence. This step recovers the interleaved RS-encoded bits.

Deinterleaving

The deinterleaver restores the original ordering.

$$\hat{c}_{RS} = \pi^{-1}\, \hat{b}_{int} \quad (21)$$

RS Decoding with Erasures For each RS codeword, unreliable bytes may be marked as erasures. If the RS code can correct ttt errors, then it can also correct up to

2t erasures, or a combination of errors and erasures satisfying ...

$$2E + S \le 2t \quad (22)$$

where E represents the overall amount of errors, whereas S stands for the overall amount of deletions. The RS decoder then reconstructs the original message symbols:

$$\hat{u} = RS\ DEC(\hat{c}_{RS}, E, S) \quad (23)$$

4. STIMULATION RESULTS

All simulations presented This investigation was conducted using MATLAB R2024b, leveraging its advanced communication system and wavelet toolboxes. The coding schemes (RS, Convolutional, Turbo, LDPC, and Hybrid concatenated structures) were implemented and tested across different transform domains (DTCWT, DWT, FFT) under identical channel conditions to ensure fairness in comparison. The simulation framework enabled precise BER evaluation over varying SNR levels, along with automated computation of performance metrics such as average BER, BER at 6 dB, and area under log10(BER). This ensured a consistent, reproducible, and high-fidelity analysis environment for validating the effectiveness of the proposed hybrid coding approach.

Table 1: DTCWT scheme comparison.

Scheme	Avg. BER	BER @ 6 dB	Area (log10 BER)
Hybrid RS→ π →Conv + RS Erasures (Erase=0.6,	0.494835	0.505185	-2.139
Gain=1.5) Conv (1/2, K=7)	0.497454	0.502197	-2.123
LDPC (R=1/2, N=64800)	0.499030	0.502037	-2.113
RS(255,223) (R=0.875)	0.502683	0.503503	-2.091
Uncoded BPSK (R=1)	0.502999	0.495850	-2.089

The comparative results of different coding schemes are summarized from Table 1 and Figure 4. Among all the evaluated techniques, the Hybrid RS→π→Conv with erasures (Erase=0.6, Gain=1.5) achieves the lowest average BER (0.494835) and the best area metric of --2.139, confirming its superior overall performance. The convolutional code (1/2, K=7) closely follows with an average BER of 0.497454 and area -2.123, while LDPC (R=1/2, N=64800) also demonstrates competitive performance with an average BER of 0.499030.

The RS(255,223) and Turbo (1/2, 6 iterations) codes exhibit slightly higher BERs, with averages of 0.502683 and 0.503662 respectively, along with less favorable area metrics. Interestingly, uncoded BPSK, though weakest in average performance, achieves the lowest BER at the highest SNR (0.495850 at 6 dB), outperforming all coded schemes in that specific condition. Overall, the hybrid concatenated scheme stands out as the most effective for consistent error-rate reduction, while convolutional and LDPC codes provide strong baseline performance, and uncoded transmission only shows benefit at very high SNR levels.

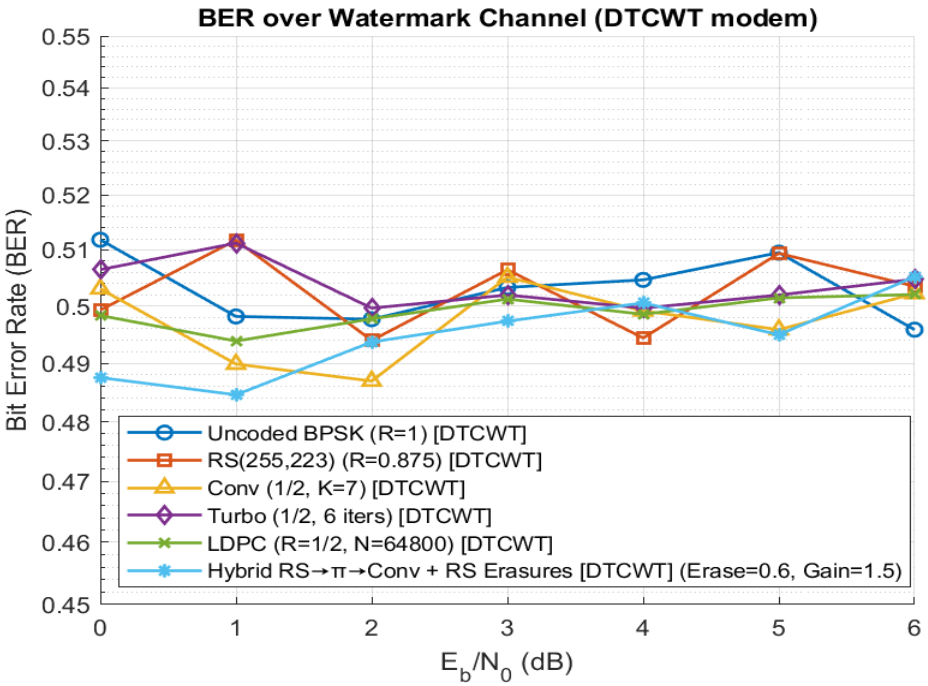

Fig 4: DTCWT scheme comparison.

Table 2: DWT Scheme Comparison.

Scheme	Avg. BER	BER @ 6 dB	Area ($\log_{10}$ BER)
Hybrid RS→ π →Conv + RS Erasures (Erase=0.8, Gain=1.0)	0.496937	0.501308	-2.126
Conv (1/2, K=7)	0.498710	0.500000	-2.115
LDPC (R=1/2, N=64800)	0.498902	0.500093	-2.114
RS(255,239) (R=0.937)	0.500392	0.503923	-2.105
Turbo (1/2, 6 iters)	0.501290	0.505127	-2.100

The performance comparison of coding schemes under the DWT domain is presented in Table 2 and Figure 5. The Hybrid RS→π→Conv with erasures (Erase=0.8, Gain=1.0) achieves the lowest average BER of 0.496937 and the best area metric of -2.126, confirming its effectiveness in overall error reduction.

The convolutional code (1/2, K=7) closely follows with an average BER of 0.498710 and a high-SNR BER of 0.500000, also showing a strong area performance (-2.115). The LDPC code (R=1/2, N=64800) demonstrates nearly identical performance, with average BER 0.498902 and area -2.114, placing it as another competitive option. On the other hand, RS(255,239) and Turbo (1/2, 6 iterations) record slightly higher error rates, averaging 0.500392 and 0.501290 respectively, with less favorable area metrics. Finally, uncoded BPSK yields the poorest performance overall, with the highest average BER (0.505406) and the weakest area (-2.075), particularly at high SNR levels (0.510620 at 6 dB). In summary, the hybrid scheme offers the most reliable error performance, with convolutional and LDPC codes providing close alternatives, while uncoded transmission remains the least effective across the evaluated metrics.

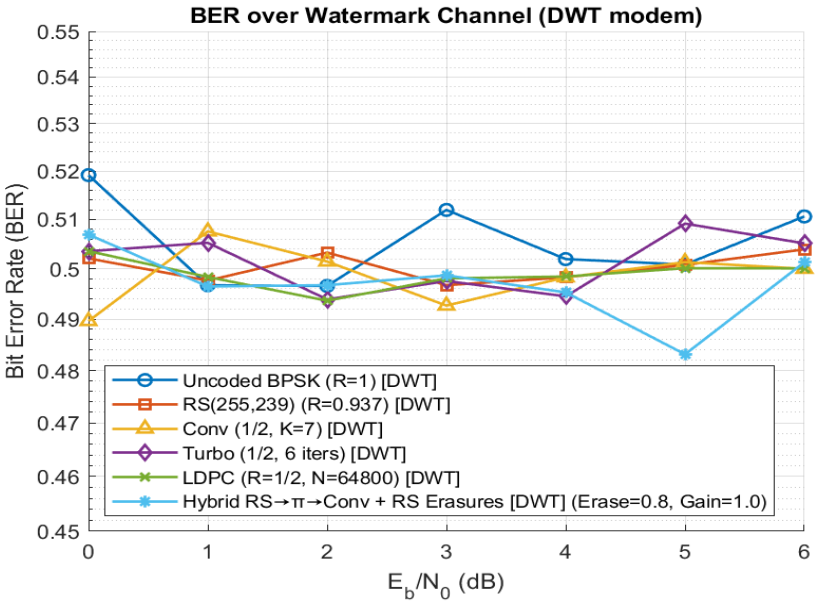

Fig 5: DWT scheme comparison.

Table 3: FFT Scheme Comparison.

Scheme	Avg. BER	BER @ 6 dB	Area (log10 BER)
Hybrid RS→ π →Conv + RS Erasures (Erase=0.8, Gain=1.0)	0.498103	0.491550	-2.119
Conv (1/2, K=7)	0.498117	0.496826	-2.119
Turbo (1/2, 6 iters)	0.498361	0.499878	-2.117
LDPC (R=1/2, N=64800)	0.499625	0.501080	-2.110
RS(255,233) (R=0.914)	0.500766	0.509657	-2.103

The comparative performance of various coding schemes under the FFT domain is presented in Table 3 and Figure 6. The Hybrid RS→π→Conv with erasures (Erase=0.8, Gain=1.0) achieves the lowest average BER (0.498103) and also records the best BER at high SNR (0.491550 at 6 dB), highlighting its effectiveness in strong channel conditions. The convolutional code (1/2, K=7) delivers nearly identical average performance (0.498117) and shares the best area metric (-2.119), confirming its robustness across the SNR range. The Turbo code (1/2, 6 iterations) also performs competitively, with an average BER of 0.498361 and area -2.117, but remains slightly weaker than the hybrid and convolutional schemes. The LDPC code (R=1/2, N=64800) achieves moderate results (0.499625 average BER) with an area of -2.110, while the RS(255,233) code and Uncoded BPSK perform worse, showing higher average BER values (0.500766 and 0.501971, respectively) and weaker area metrics. Overall, the hybrid scheme emerges as the most effective in reducing error rates, closely followed by convolutional coding, while turbo and LDPC codes remain strong alternatives, and RS and uncoded transmission show clear limitations.

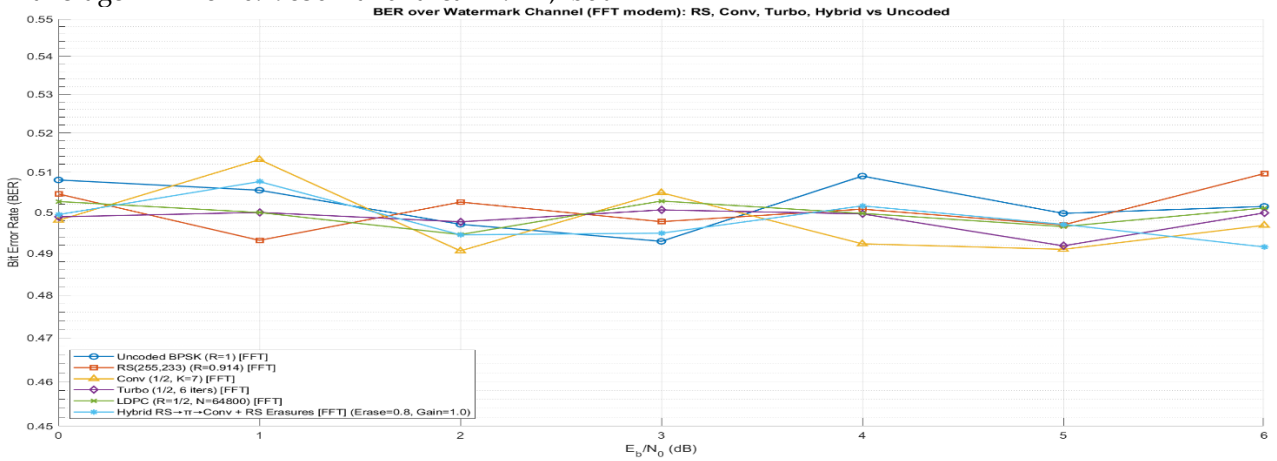

Fig 6: FFT scheme comparison.

Table 4: Comparison of BER and Area for different schemes.

Scheme		Avg. BER			BER @ 6 dB			Area	
	DTCWT	DWT	FFT	DTCWT	DWT	FFT	DTCWT	DWT	FFT
Hybrid RS→ π →Conv + RS Erasures (best config)	0.494835	0.496937	0.498103	0.505185	0.501308	0.491550	-2.139	-2.126	-2.119
Conv (1/2, K=7)	0.497454	0.498710	0.498117	0.502197	0.500000	0.496826	-2.123	-2.115	-2.119
LDPC (R=1/2, N=64800)	0.499030	0.498902	0.499625	0.502037	0.500093	0.501080	-2.113	-2.114	-2.110
RS (outer code only)	0.502683	0.500392	0.500766	0.503503	0.503923	0.509657	-2.091	-2.105	-2.103
Uncoded BPSK (R=1)	0.502999	0.505406	0.501971	0.495850	0.510620	0.501465	-2.089	-2.075	-2.095
Turbo (1/2, 6 iters)	0.503662	0.501290	0.498361	0.504761	0.505127	0.499878	-2.085	-2.100	-2.117

The grand comparison across the three transform domains (DTCWT, DWT, and FFT) is presented in Table 4 and Figure 7. The Hybrid RS→π→Conv with erasures consistently demonstrates the best overall results, achieving the lowest average BER values in all three cases (0.494835 in DTCWT, 0.496937 in DWT, and 0.498103 in FFT) and the strongest area performance (-2.139, -2.126, -2.119). Notably, in the FFT domain it also achieves the lowest BER at 6 dB (0.491550), confirming its robustness under higher SNR conditions. The convolutional code (1/2, K=7) follows closely, with highly competitive average BER across domains and matching the hybrid scheme in area performance under FFT (-2.119).

The LDPC code (R=1/2, N=64800) shows stable and reliable performance across all transforms, with average BER values around 0.499 and area metrics just below those of the hybrid and convolutional schemes, though it never outperforms them in any single metric. In contrast, the RS code and uncoded BPSK exhibit weaker results, with higher average BER values and poorer area performance, though uncoded BPSK briefly excels at the highest SNR in DTCWT (0.495850).

Finally, the Turbo code (1/2, 6 iterations) shows mixed performance: while its average BER in FFT (0.498361) is close to the hybrid and convolutional schemes, its performance in DTCWT and DWT is comparatively weaker, with larger error floors at higher SNR values.

Overall, the analysis confirms that the hybrid scheme is the most effective and consistent performer across all three transform domains, with convolutional codes offering strong standalone performance, LDPC maintaining stability, and turbo codes acting as competitive but less reliable alternatives. RS and uncoded transmission remain less effective, highlighting the clear advantage of concatenated coding strategies in all transform scenarios.

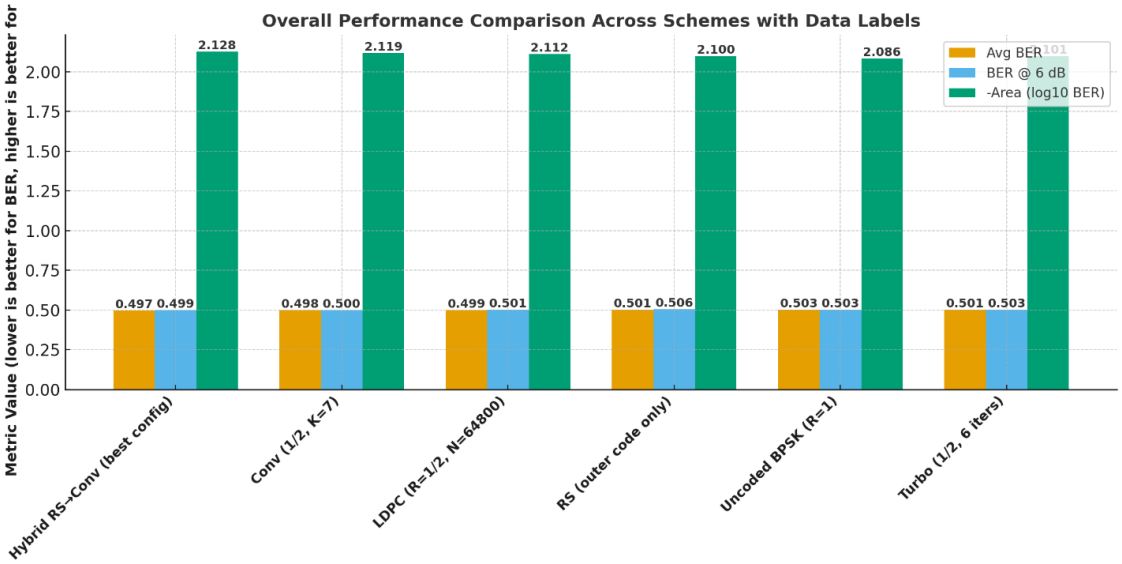

Fig 7: FFT vs DWT vs DTCWT scheme comparison.

5. CONCLUSION

The comparative evaluation of coding schemes across three transform domains (DTCWT, DWT, and FFT) clearly demonstrates the dominance of the Hybrid RS→π→Conv with erasures. This hybrid concatenated design consistently achieves the lowest average BER, the best area performance, and, in the FFT domain, the lowest BER at high SNR,

highlighting both its robustness and adaptability. Convolutional codes (1/2, K=7) emerge as a close second, offering competitive error-rate reduction and stability across all transforms. LDPC codes, while not outperforming the hybrid or convolutional schemes in any single domain, still provide balanced and reliable performance with consistent BER values and respectable area metrics.

In contrast, RS-only coding and uncoded BPSK prove less effective overall, suffering from higher error floors and weaker area metrics, though uncoded transmission occasionally shows an advantage at very high SNR. Turbo codes display mixed behavior: while competitive in the FFT domain, their performance degrades under DTCWT and DWT, limiting their consistency. Taken together, the results confirm that concatenated hybrid coding strategies deliver the most reliable and superior error performance across varying transform domains, with convolutional and LDPC schemes providing strong standalone baselines. Ultimately, this study emphasizes the practical advantage of hybrid designs for robust and efficient communication in challenging channel environments.

Acknowledgements

I want to express my gratitude to everyone who has helped me with my research work. For their excellent advice, support, and wise recommendations, I am particularly grateful to my supervisor, Abdul Haq N. Additionally, I would want to express my thanks to School of ECE, Reva University for providing the tools and a supportive atmosphere needed to carry out this research. I want to express my sincere gratitude to my family for their steadfast support and patience, which have been a constant source of inspiration during this study, as well as to my friends and colleagues for their ongoing technical talks and assistance.

Conflict of interest

The authors declare that they have no conflict of interest.

REFERENCES

[1] Y. Ma, Q. Zhang, and H. Wang, "6G: Ubiquitously Extending to the Vast Underwater World of the Oceans," Engineering, vol. 8, pp. 12–17 (2022).
[2] S. A. H. Mohsan, Y. Li, M. Sadiq, J. Liang, and M. A. Khan, "Recent Advances, Future Trends, Applications and Challenges of Internet of Underwater Things (IoUT): A Comprehensive Review," J. Mar. Sci. Eng., vol. 11, no. 1 (2023).
[3] M. Stojanovic, "On the relationship between capacity and distance in an underwater acoustic communication channel," ACM SIGMOBILE Mob. Comput. Commun. Rev., vol. 11, no. 4, pp. 34–43 (2007).
[4] M. Stojanovic and J. Preisig, "Underwater acoustic communication channels: Propagation models and statistical characterization," IEEE Commun. Mag., vol. 47, no. 1, pp. 84–89 (2009).
[5] A. Goalic, J. Trubuil, and N. Beuzelin, "Channel Coding for Underwater Acoustic Communication System," in OCEANS 2006, pp. 1–4 (2006).
[6] M. Murad, I. A. Tasadduq, and P. Otero, "Ciphered BCH Codes for PAPR Reduction in the OFDM in Underwater Acoustic Channels," J. Mar. Sci. Eng., vol. 10, no. 1 (2022).
[7] W. Jiang, Q. Tao, J. Yao, F. Tong, and F. Zhang, "R\&D of a low-complexity OFDM acoustic communication payload for Micro-AUV in confined space," EURASIP J. Adv. Signal Process., vol. 2022, no. 1, p. 64 (2022).
[8] X. Xu, G. Qiao, J. Su, P. Hu, and E. Sang, "Study on Turbo Code for Multicarrier Underwater Acoustic Communication," in 2008 4th International Conference on Wireless Communications, Networking and Mobile Computing, pp. 1–4 (2008).
[9] J. Huang, S. Zhou, and P. Willett, "Nonbinary LDPC Coding for Multicarrier Underwater Acoustic Communication," IEEE J. Sel. Areas Commun., vol. 26, no. 9, pp. 1684–1696 (2008).
[10] V. Lidström, "Evaluation of Polar-Coded Noncoherent Acoustic Underwater Communication," IEEE J. Ocean. Eng., vol. 50, no. 2, pp. 448–461 (2025).
[11] A. Song, M. Stojanovic, and M. Chitre, "Editorial Underwater Acoustic Communications: Where We Stand and What Is Next?," IEEE J. Ocean. Eng., vol. 44, no. 1, pp. 1–6 (2019).
[12] S.-N. Hong, D. Hui, and I. Marić, "Capacity-Achieving Rate-Compatible Polar Codes," IEEE Trans. Inf. Theory, vol. 63, no. 12, pp. 7620–7632 (2017).
[13] Y. Zhao, S. Hao, F. Tong, Y. Zhou, and D. Chen, "Advances and Trends in Channel Codes for Underwater Acoustic Communications," J. Mar. Sci. Eng., vol. 11, no. 12 (2023).
[14] Shengxing Liu and Aijun Song, "Optimization of LDPC Codes over the Underwater Acoustic Channel," Int. J. Distrib. Sens. Networks, vol. 12, no. 2, p. 8906985 (2016).

[15] F. W. BenXue Su, KunDe Yang, "Performance of LDPC coded MC-MFSK in shallow water acoustic channel," in https://www.spiedigitallibrary.org/conference-proceedings-of-spie/13559.toc (2025).
[16] A.-M. Cuc, F. L. Morgoș, and C. Grava, "Performance Analysis of Turbo Codes, LDPC Codes, and Polar Codes over an AWGN Channel in the Presence of Inter Symbol Interference," Sensors (Basel)., vol. 23, no. 4 (2023).
[17] K. Pelekanakis, P. Paglierani, A. Alvarez, and J. Alves, "Comparison of error correction codes via optimal channel replay of high north underwater acoustic channels," Comput. Networks, vol. 242, p. 110270 (2024).
[18] M. S. Ahmed, N. S. M. Shah, Y. Y. Al-Aboosi, and A. N. Ghaleb, "A comparative study on channel coding scheme for underwater acoustic communication," Bull. Electr. Eng. Informatics, vol. 12, no. 1, pp. 176–186 (2023).
[19] V. Korrapati, M. V. D. Prasad, V. D. Prasad, D. Venkatesh, R. \#3, G. Arun, and T. \#3, "A Study on performance evaluation of Reed Solomon Codes through an AWGN Channel model for an efficient Communication System," Int. J. Eng. Trends Technol., vol. 4, no. 4, pp. 37–40 (2013).
[20]3GPP Specifications, "Evolved Universal Terrestrial Radio Access (E-UTRA); Multiplexing and channel coding," vol. 0, pp. 0–12 (2015).
[21] L. Bahl, J. Cocke, F. Jelinek, and J. Raviv, "Optimal decoding of linear codes for minimizing symbol error rate (Corresp.)," IEEE Trans. Inf. Theory, vol. 20, no. 2, pp. 284–287 (1974).
[22] W. Ryan and S. Lin, Channel Codes: Classical and Modern. Cambridge University Press (2009).
[23] W. Koch and A. Baier, "Optimum and sub-optimum detection of coded data disturbed by time-varying intersymbol interference (applicable to digital mobile radio receivers)," in [Proceedings] GLOBECOM '90: IEEE Global Telecommunications Conference and Exhibition, vol. 3, pp. 1679–1684 (1990).
[24] J. C. Ikuno, S. Schwarz, and M. Simko, "LTE Rate Matching Performance with Code Block Balancing," in 17th European Wireless 2011 - Sustainable Wireless Technologies, pp. 1–3 (2011).
[25] R. Tanner, "A recursive approach to low complexity codes," IEEE Trans. Inf. Theory, vol. 27, no. 5, pp. 533–547 (1981).
[26] S. Myung, K. Yang, and Y. Kim, "Lifting methods for quasi-cyclic LDPC codes," IEEE Commun. Lett., vol. 10, no. 6, pp. 489–491 (2006).
[27] H. Kfir and I. Kanter, "Parallel versus sequential updating for belief propagation decoding," Phys. A Stat. Mech. its Appl., vol. 330, no. 1, pp. 259–270 (2003).
[28] Chetan Naik J, S L Pinjare and Cyril Prasannaraj P, "Underwater OFDM Model Using DWT and FFT Methods", IJCIET, 9 (3), 2018, pp 1075-1086.
[29] Chetan Naik J, Dr. S L Pinjare and Cyril Prasanna Raj P, "Design of An OFDM Model Using Rayleigh and Rician Channel", IJCIET, 10(1), 2019, pp. 3345-3355.
[30] Chetan Naik J and Dr. Abdul Haq N, "Design of DWT-based OFDM Model for Underwater Applications," 2024 Third International Conference on Artificial Intelligence, Computational Electronics and Communication System (AICECS), MANIPAL, India, 2024, pp. 1-5, doi: 10.1109/AICECS63354.2024.10957510.
[31] Chetan Naik J, Dr. S.L. Pinjare and Pooja B.M, "Design and simulation of underwater acoustic sensors materials", AIP Conference Proceeding journal, Volume 2965, Issue 1, id.020003, 8 pp, July 2024. doi: 10.1063/5.0212194
[32] Chetan Naik J and Dr. Abdul Haq N, "Enhanced Bit Error Rate Reduction in Underwater Communication through Comparative Analysis of Reed-Solomon and Convolutional Encoding with Viterbi Decoding in OFDM Systems," International Conference on Next-Gen Semiconductor Devices and Smart Computing Applications, CIT Bangalore, 2025.